Sequential Activation of Microglia and Astrocyte Cytokine Expression Precedes Increased Iba-1 or GFAP Immunoreactivity following Systemic Immune Challenge

Diana M. Norden[1,*], **Paige J. Trojanowski**[1,*], **Emmanuel Villanueva**[1], **Elisa Navarro**[1], and **Jonathan P. Godbout**[1,2,3]

[1]Department of Neuroscience, The Ohio State University, 333 W. 10th Ave, Columbus, OH 43210, USA.

[2]Institute for Behavioral Medicine Research, The Ohio State University, 460 Medical Center Dr., Columbus, OH 43210, USA.

Abstract

Activation of the peripheral immune system elicits a coordinated response from the central nervous system. Key to this immune to brain communication is that glia, microglia and astrocytes, interpret and propagate inflammatory signals in the brain that influence physiological and behavioral responses. One issue in glial biology is that morphological analysis alone is used to report on glial activation state. Therefore, our objective was to compare behavioral responses after *in vivo* immune (lipopolysaccharide, LPS) challenge to glial specific mRNA and morphological profiles. Here, LPS challenge induced an immediate but transient sickness response with decreased locomotion and social interaction. Corresponding with active sickness behavior (2–12h), inflammatory cytokine mRNA expression was elevated in enriched microglia and astrocytes. Although pro-inflammatory cytokine expression in microglia peaked 2–4 h after LPS, astrocyte cytokine and chemokine induction was delayed and peaked at 12 h. Morphological alterations in microglia (Iba-1$^+$) and astrocytes (GFAP$^+$), however, were undetected during this 2–12 h timeframe. Increased Iba-1 immunoreactivity and de-ramified microglia were evident 24 and 48 h after LPS but corresponded to the resolution phase of activation. Morphological alterations in astrocytes were undetected after LPS. Additionally, glial cytokine expression did not correlate with morphology after four repeated LPS injections. In fact, repeated LPS challenge was associated with immune and behavioral tolerance and a less inflammatory microglial profile compared to acute LPS challenge. Overall, induction of glial cytokine expression was sequential, aligned with active sickness behavior, and preceded increased Iba-1 or GFAP immunoreactivity after LPS challenge.

Keywords

neuroinflammation; microglia; astrocytes; lipopolysaccharide; sickness behavior

[3]Corresponding author: J.P. Godbout, 259 IBMR Bldg, 460 Medical Center Dr., The Ohio State University, Columbus, OH 43210, USA. Tel: (614) 293-3456 Fax: (614) 366-2097, jonathan.godbout@osumc.edu.
*Authors contributed equally to the manuscript

Introduction

Microglia are innate immune cells and are involved in immune surveillance within the central nervous system (CNS) (Davalos et al., 2005). For instance, peripheral lipopolysaccharide (LPS) challenge activates the innate immune system, which uses several neural and humoral pathways to communicate with the neurovascular unit (endothelium), brain stem, and circumventricular organs of the brain (Ching et al., 2007; Hansen et al., 2001; Lacroix et al., 1998; Laflamme et al., 1999). This communication results in the propagation of cytokines and chemokines within the brain by microglia (Chen et al., 2012; Henry et al., 2009). The activation profile detected is consistent with a M1 profile of microglia and macrophages (Mosser and Edwards, 2008). Cytokine induction by microglia, including IL-1β, TNFα and IL-6, helps to propagate this immune derived signal within the brain and mediate physiological and behavioral responses (Dantzer, 2001; Dantzer et al., 2008). Chemokine induction by active microglia also transmits neuroinflammatory signals and may represent a mechanism by which resident microglia signal to peripheral immune cells (Carson et al., 2006; Cazareth et al., 2014; Fenn et al., 2014b; Puntambekar et al., 2011; Wohleb et al., 2013). In addition, microglial activation following immune challenge is associated with an acute phase response, which involves reduced iron bioavailability to limit pathogen growth and prevent excess CNS damage after injury (Parrow et al., 2013; Sauerbeck et al., 2013). Collectively, peripheral immune challenge elicits transient neuroinflammation, which is mediated by microglia, and represents a coordinated response between the immune system and brain.

Because of the inflammatory capacity of microglia, these cells are under tight regulation provided by anti-inflammatory cytokines, neuropeptides, and hormones (Biber et al., 2007; Rivest, 2009). This regulation ensures that activated microglia return to a surveying state after the resolution of immune challenge (Norden and Godbout, 2013). While there is considerable interest in M1 and M2 (regulation/repair) phases of activation (Mosser and Edwards, 2008), it is unclear if a shift from this M1 to M2 profile is required as inflammation resolves after immune challenge (Fenn et al., 2012). Another related issue in the exploration of microglial activation phases is the reliance on Iba-1 immunoreactivity to report on their activation state. While microglia undergo cytoskeletal rearrangements that alter their morphology (Davalos et al., 2005), these morphological changes may not accurately represent an "active" inflammatory profile. For example, in a model of prion disease, LPS injection increased cytokine expression in microglia independent of significant differences in microglial morphology (Cunningham et al., 2005b).

Astrocytes are also active participants in propagating and regulating neuroinflammation (Farina et al., 2007; Liu et al., 2011; Norden et al., 2014a). Astrocytes are activated by inflammatory mediators and cytokines, including IL-1β (Carpentier et al., 2005; John et al., 2004). Activated astrocytes produce many regulatory factors that may influence CNS immunity and provide negative feedback to activated microglia (Min et al., 2006). Thus, a secondary phase of activation mediated by astrocytes helps to regulate microglial responses after immune challenge. In this regard, microglia and astrocytes both contribute to acute phase, inflammatory, and regulatory responses after peripheral immune challenge. Similar to assessing microglial activation by morphology, activation states of astrocytes are determined

based on increased GFAP labeling. Although the inflammatory potential of astrocytes has been assessed after CNS trauma (Myer et al., 2006; Sofroniew, 2005; Voskuhl et al., 2009), the activation profile of astrocytes during peripheral immune challenge is less understood.

One consequence of microglia and astrocyte activation after peripheral immune challenge with LPS is the induction of sickness behavior. Propagation of cytokines and secondary signals leads to physiological and behavioral components of the sickness response, including decreased activity and reduced social interaction (Dantzer et al., 2008). These behavioral changes are evolutionarily adaptive and necessary to reallocate the host's resources and to fight infection (Berg et al., 2004; Bluthe et al., 2000a). Recent studies also indicate that repeated LPS injections enhance neuroprotective properties of microglia during traumatic CNS injury, further extending the interest in understanding glial activation profiles (Chen et al., 2014; Chen et al., 2012). Overall, a single or repeated LPS i.p. injection can be used to examine the biochemical and morphological profiles of astrocytes and microglia in the context of functional behavioral responses.

The aim of this study was to compare behavioral responses after LPS challenge to glia specific levels of cytokine expression and morphology. We show that increased pro-inflammatory cytokine expression by microglia correlated with active sickness behavior. De-ramification of microglia and increased Iba-1 immunoreactivity, however, was delayed following the LPS injection and corresponded with the resolution phase of microglial activation. While mRNA profiling also detected astrocyte activation after LPS challenge, morphological alterations in astrocytes (GFAP immunoreactivity) were not detected at any time. Repeated LPS injection also increased Iba-1 immunoreactivity that corresponded with the resolution of microglial activation.

Materials and Methods

Mice

Adult (3–4 months-old) BALB/c mice were obtained from our breeding colony kept and in barrier-reared conditions in a specific-pathogen-free facility at The Ohio State University. Mice were individually housed in polypropylene cages and maintained at 25° C under a 12 h light/12 h dark cycle with *ad libitum* access to water and rodent chow. All procedures were in accordance with the National Institute of Health Guidelines for the Care and Use of Laboratory Animals and approved by The Ohio State University Institutional Laboratory Animal Care and Use Committee.

Peripheral injection of LPS

In the first set of studies, adult mice received a single intraperitoneal (i.p.) injection of either saline or 10 μg LPS (approximately 0.33 mg/kg). The LPS dosage was selected because it elicits a pro-inflammatory cytokine response in the brain resulting in a transient sickness response in adult mice (Berg et al., 2004; Godbout et al., 2005). In the second set of studies, adult mice received either a single or four repeated (i.p.) injections of saline or 20 μg LPS (approximately 0.66 mg/kg). For repeated LPS challenge, mice received one injection of LPS every 24 h for four consecutive days. This LPS dosage and time course were selected

because they are similar to previous studies that have administered multiple injections to investigate microglial activation profiles (Bodea et al., 2014; Cardona et al., 2006; Chen et al., 2012; Puntener et al., 2012).

Locomotor activity

Mice were recorded in their home cage for 5 minutes. On the video records, cages were divided into 6 identical virtual rectangles, and the number of line crossings was determined during the last 3 minutes. Baseline locomotor activity was measured prior to experimental treatment (time 0).

Social exploratory behavior

Social exploratory behavior was determined as a measure of sickness behavior as previously described (Godbout et al., 2005). A novel juvenile was introduced into the test subject's home cage for 10 min and the cumulative amount of time the experimental subject engaged in social investigation of the juvenile (e.g., anogenital sniffing, trailing) was determined. Baseline social behavior was measured prior to experimental treatment (time 0). Results are expressed as the percent of time engaged in social behavior compared to baseline.

Microglia and astrocyte isolation from brain

Microglia and astrocytes were isolated from brain homogenates using a Percoll density gradient as previously described (Henry et al., 2009; Norden et al., 2014a; Sawicki, 2014). In brief, the brain was homogenized and cell pellets were re-suspended in 70% isotonic Percoll. A discontinuous Percoll density gradient (70%, 50%, 35%, 0%) was layered and centrifuged for 20 min at 2000×g. Enriched microglia were collected from the interphase between 70% and 50% Percoll, with approximately 90% purity (CD11b$^+$/ CD45^{low}). Less than 1.5% of the enriched cells were CD11b$^+$/ CD45^{high} macrophages. Enriched astrocytes were collected from the interphase between 50% and 35% Percoll, with approximately 70% purity (CD11b^{neg}/GLAST-1$^+$). There was no contamination of endothelial cells (CD31$^+$) in either Percoll gradient used for glia separation (data not shown).

Immunohistochemistry and digital image analysis

Mice were deeply anesthetized and transcardially perfused with PBS followed by 4% formaldehyde. Brains were post-fixed in 4% formaldehyde for 24 h and cryoprotected in 20% sucrose in PBS for 48 h. Preserved brains were frozen using dry-ice cooled isopentane (−165°C) and sectioned (30 μm) using a Microm HM550 cryostat. Brain sections were identified by reference markers in accordance with the stereotaxic mouse brain atlas (Paxinos and Franklin, 2004). Iba-1 or GFAP staining was performed as previously described (Fenn et al., 2014a). In brief, free-floating sections were blocked and then incubated with rabbit anti-mouse Iba-1 antibody (Wako Chemicals) or rabbit anti-mouse GFAP antibody (Dako) overnight at 4°C. Sections were washed with PBS and incubated with Alexa Flour 488/594 secondary antibodies. Sections were coverslipped using Flourmount G.

Fluorescent images were visualized using an epifluorescent Leica DM5000B microscope and captured using a Leica DFC300 FX camera and imaging software. Digital image

analysis (DIA) (Donnelly et al., 2009) of Iba-1 or GFAP staining was used to quantify the phenotypic changes of microglia (frontal cortex and hippocampus) and astrocytes (hippocampus). For each mouse, 4–6 representative images (20×) were taken of the PFC, and 10–12 representative images (20×) were taken in the dentate gyrus, CA1, and CA3 regions of the hippocampus. A threshold for positive staining was determined for each image that included all cell bodies and processes, but excluded background staining (ImageJ). Results were reported as the average percent area in the positive threshold for all representative pictures.

Determination of IL-6 protein levels in plasma

IL-6 was determined from plasma using the BD OptEIA Mouse IL-6 ELISA according to the manufacturer's instructions (BD Biosciences). In brief, 96-well enzyme immunoassay plates were coated with anti-mouse IL-6 capture antibody and incubated overnight at 4°C. Samples and standards were added and incubated for 2 h followed by biotinylated anti-mouse IL-6 antibody for 2 h. Reactions were exposed using streptavidin-horseradish peroxidase conjugate followed by tetramethylbenzidine liquid substrate. Reactions were terminated and absorbance was read at 450 nm using a Synergy HT Plate Reader (Bio-tek instruments). The assay was sensitive to 10 ng/ml IL-6 and the interassay and intra-assay coefficients of variation were less than 10%.

RNA isolation and RT-PCR

RNA was isolated from a 1 mm coronal brain section using the Tri-Reagent protocol (Sigma-Aldrich). For Percoll enriched microglia and astrocytes, RNA was isolated using the PrepEase kit (USB, CA). RNA was reverse transcribed to cDNA and real-time (RT)-PCR was performed using the Applied Biosystems Taqman® Gene Expression Assay-on-Demand Gene Expression protocol. Target cDNA (e.g., IL-1β, IL-6) and reference cDNA (glyceraldehyde-3-phosphate dehydrogenase; GAPDH) were amplified simultaneously using an oligonucleotide probe with a 5' fluorescent reporter dye (6-FAM). Fluorescence was determined on an ABI PRISM 7300-sequence detection system (Applied Biosystems). Data were analyzed using the comparative threshold cycle (Ct) method and results are expressed as fold difference.

Statistical Analysis

To ensure a normal distribution, data were subjected to the Shapiro-Wilk test using Statistical Analysis Systems (SAS) statistical software (Cary, NC). To determine significant main effects and interactions between main factors, single LPS injection data were analyzed using one-way (i.e., Saline and LPS) or two-way (i.e., LPS × Time) ANOVA using the General Linear Model procedures of SAS. Repeated LPS injection data were analyzed using one-way (i.e., Saline and LPS 1× and LPS 4×) or two-way (Group × Time) ANOVA using the General Linear Model procedures of SAS. When appropriate, differences between treatment means were evaluated by an *F*-protected *t*-test using the Least-Significant Difference procedure of SAS. All data are expressed as treatment means ± standard error of the mean (SEM). Values were considered to be significantly different at *p*-values < 0.05 and a tendency at *p*-values = 0.06 to 0.1.

Results

Acute LPS challenge promoted a transient sickness response that was resolved within 48 h

In glial biology, analysis of morphology is commonly used as a single measure to report on the activation state of microglia (de-ramification, Iba-1 labeling) and astrocytes (astrogliosis, GFAP labeling). Morphological analysis alone may not be a reliable index of inflammatory profile, especially in the context of activation profiles and their influence on behavioral or physiological processes. Therefore, the objective of this study was to temporally compare behavioral responses after LPS challenge to glial specific levels of cytokine expression and morphological profiles.

In the first study, adult male BALB/c mice were injected i.p. with LPS (10 μg), and several indices of sickness behavior (e.g., weight loss, lethargy, social interaction) were determined over a 72 h time course. Fig.1A shows that single i.p. injection of LPS reduced body weight in a time dependent manner ($F_{(5,71)}$=7.27, p<0.001). Body weight was reduced by 4 h after LPS (p<0.01) and mice continued to lose body weight through 48 h. LPS challenge also decreased locomotor activity in a time dependent manner ($F_{(6,87)}$=7.33, p<0.001, Fig.1B). For example, LPS injection initially reduced locomotor activity (2–12 h post injection, p<0.001), but locomotion steadily increased after 12 h and reached baseline activity by 72 h. LPS injection had a similar time dependent effect on social exploratory behavior ($F_{(6,74)}$=5.71, p<0.001, Fig.1C). Social exploratory behavior was most reduced between 2 and 4 h following LPS (p<0.001, for each) and returned to baseline levels by 24 h. Overall, acute injection of LPS induced an active sickness response in which mice recovered to baseline social exploration by 24 h and baseline locomotor activity by 48 h.

LPS injection causes the acute phase response with the release of inflammatory cytokines into circulation, including IL-6 (Skelly et al., 2013). Therefore, IL-6 was determined in the plasma of mice used in the behavioral studies above. Fig.1D shows increased IL-6 in the plasma 2–12 h after LPS challenge (p<0.02). IL-6 levels returned to baseline by 24 h after LPS and were undetectable 48 and 72 h after LPS (data not shown). Thus, there is a transient increase in plasma IL-6 after peripheral LPS injection.

Acute LPS challenge induced concomitant induction of inflammatory, regulatory, and acute phase markers in the brain

To assess the overall inflammatory status of the brain, a coronal brain section was collected during a similar time course as the sickness behavior (2, 4, 12, 24, and 48 h after LPS injection). In these samples, mRNA expression of several inflammatory (IL-1β, IL-6, and TNFα), regulatory (IL-4Rα, IL-10, YM-1, TGFβ), and acute phase genes (Serum amyloid 3, Ceruloplasmin, Haptoglobin) was determined (Table 1).

The mRNA levels of two markers associated with the identification of microglia (Iba-1) or astrocytes (GFAP) were determined. Iba-1 expression was increased in the brain 24 h after LPS (p<0.01) and GFAP expression was increased 12–24 h after LPS (p<0.01). Overall, the induction of these markers was modest and not detectable until 24 h after LPS.

There was a significant increase in mRNA levels of IL-1β, IL-6, TNFα beginning at 2 h and continued through 4 h for IL-6 and 12 h for both IL-1β and TNFα ($p<0.05$). Two of the regulatory genes had a rapid induction and two had a delayed induction after LPS. Induction of IL-10 mRNA began at 2 h ($p<0.01$), but these levels returned to baseline by 12 h. IL-4Rα was also increased by 2 h ($p<0.03$) and was maintained for 12 h after LPS ($p<0.01$). The induction of the other two regulatory genes associated with an M2 microglial phenotype, TGFβ and YM-1, however, was delayed until 12–24 h after LPS ($p=0.1$). These data are consistent with previous findings that astrocytes increase TGFβ mRNA expression during resolution of inflammation following LPS (Norden et al., 2014a).

The acute phase proteins Saa3, CerulP, and HaptoG followed a similar time course. Saa3 was induced at 4 h ($p=0.1$), peaked at 12 h ($p<0.01$) and remained elevated 24 h after LPS ($p<0.05$). CerulP and HaptoG were increased by 4 h after LPS ($p<0.01$) and were maintained 24 h later ($p=0.08$). Overall, inflammatory, regulatory, and acute phase genes were all enhanced in the brain by 4 h after LPS. Notably, TGFβ, YM-1, and Saa3 had a delayed induction after LPS and were still elevated 24 h later.

Rapid microglial cytokine induction after acute LPS challenge preceded astrocyte cytokine expression

We next sought to determine the mRNA profiles of astrocytes and microglia over a 48 h time course after a single LPS challenge. Microglia and astrocytes were isolated and enriched using a Percoll density gradient (Fig.2A) and mRNA levels of several pro-inflammatory genes (IL-6, IL-1β, TNFα, CCL2) and anti-inflammatory genes (IL-10 and TGFβ) were determined.

Fig.2B shows representative bivariate dot plots of CD11b and CD45 labeling of Percoll enriched microglia and CD11b and Glast-1 labeling of Percoll-enriched astrocytes. As we have previously reported (Henry et al., 2009; Norden et al., 2014a), isolation from the 70–50 interphase preferentially enriched (over 85%) for microglia (CD11b$^+$/CD45^{low}). CNS macrophages (CD45^{high}) were also present in the 70–50 interphase of Percoll but were less than 2% and this percentage was not influenced by LPS injection. Furthermore, isolation from the 50–35 interphase of Percoll preferentially enriched (over 70%) for astrocytes (CD11b-/Glast-1) and this percentage was not influenced by LPS injection.

In enriched microglia, there was a rapid response to LPS with mRNA induction of several pro-inflammatory genes including IL-6, IL-1β, and TNFα ($F_{(5,40)}=6.78$, $p<0.001$, for each). Fig.2C shows an initial and peak 10-fold induction of IL-6 at 2 h ($p<0.01$) that was maintained at 4 h ($p<0.01$) but back to baseline expression by 12 h. Likewise, IL-1β mRNA induction in enriched microglia was robustly increased 40-fold at 2 h after LPS ($p<0.01$) and 80-fold at 4 h ($p<0.01$, Fig.2D). Microglial IL-1β expression remained elevated 12 h after LPS ($p<0.05$) but was back to baseline by 24 h. Levels of TNFα and chemokine CCL2 mRNA were also elevated by 2 h in enriched microglia ($p<0.01$, for each) and were maintained up to 12 and 24 h after LPS, respectively ($p<0.05$, Figs.2E&F). In microglia, the peak of pro-inflammatory cytokine expression occurred 2 to 4 h after LPS injection and was back to similar levels as saline injected controls by 24 h.

There was also a rapid response to LPS with induction of the anti-inflammatory cytokine IL-10 in enriched microglia. Microglial induction of IL-10 was evident by 2 h after LPS ($p<0.05$), highest at 4 h ($p<0.01$), and tended to be maintained 24 h after LPS ($p=0.10$) (Fig. 2G). TGFβ, however, was not induced in enriched microglia at any time point after LPS injection (Fig.2H). Thus, there was a concomitant induction of IL-10 mRNA in enriched microglia with pro-inflammatory mediators including IL-1β, IL-6, and TNFα.

In enriched astrocytes, LPS challenge increased the mRNA expression of several inflammatory genes in a time dependent manner (Figs.2I–K). There was a limited induction of IL-6 mRNA in enriched astrocytes that was only elevated 2 h after LPS ($p<0.01$, Fig.2I). IL-1β mRNA in astrocytes was detected by 2 h ($p<0.03$) and was highest at 12 h ($p<0.01$, Fig.2J). There was also a 15-fold induction of TNFα in enriched astrocytes 12 h after LPS ($p<0.01$, Fig.2K). This increase was maintained at 24 h ($p<0.01$), but returned to baseline expression by 48 h after LPS. Similar to the TNFα induction, there was a 20-fold induction of CCL2 in astrocytes at 12 h after LPS ($p<0.01$) that was maintained at 24 h after LPS ($p<0.01$, Fig.2L).

Enriched astrocytes did not have a significant induction of IL-10 after LPS (Fig.2M). The mRNA expression of TGFβ tended to be reduced in enriched astrocytes 2 and 4 h after LPS ($p=0.1$, Fig.2N). At 24 h after LPS, however, the expression of TGFβ was significantly increased compared to saline injected controls ($p<0.05$, Fig.2N). Taken together, the peak of pro-inflammatory cytokine and chemokine mRNA expression in enriched astrocytes occurred between 12 and 24 h after LPS injection, which was delayed compared to the robust induction of cytokines in microglia at 2–4 h.

Iba-1 immunoreactivity of microglia was increased in the cortex and hippocampus 24 and 48 h after LPS challenge while GFAP immunoreactivity of astrocytes in the hippocampus was unaffected

Here we show evidence of glial induction of cytokines within 2 h of a peripheral LPS injection that corresponded with active sickness behavior. Therefore, we next sought to determine morphological alterations in microglia and astrocytes over the same time course. It is important to note that GFAP labels astrocytes in the white matter tracts and the hippocampus of mice but does not label astrocytes in the cortex (Zhang and Barres, 2010). The hippocampus and cortex were selected for microglial morphological analysis because we and others have detected increased Iba-1 immunoreactivity in these regions after peripheral LPS challenge (Wohleb et al., 2012). Representative labeling for either Iba-1 (cortex) or GFAP (hippocampus) is shown 0, 4, 12, 24, 48 and 72 h after LPS injection (Fig. 3A&B). Fig.3A shows that LPS injection was not associated with increased Iba-1 immunoreactivity at either 4 or 12 h. In fact, these microglia had a similar Iba-1 proportional area as the saline controls (Fig.3C). At 24 and 48 h following LPS, however, microglia had larger cell bodies and thicker processes, consistent with a de-ramified morphological profile, and there was a significant increase in Iba-1 immunoreactivity ($p<0.05$, Fig.3A&C). Similar to the frontal cortex, increased Iba-1 proportional area was evident in microglia of the hippocampus 24–72 h after LPS ($p<0.05$, Fig.3D). For astrocytes, there were neither differences in morphology (Fig.3B) nor GFAP immunoreactivity at any time after LPS

injection (Fig.3E). Thus, immunoreactivity of Iba-1 was evident 24–48 h after LPS but delayed compared to the rapid cytokine mRNA induction. Although there was a detectable increase in cytokine expression in enriched astrocytes after LPS, there were no differences in GFAP labeling detected in astrocytes over the same time course.

Acute LPS challenge corresponded to a more pronounced active sickness response over 24 h compared to repeated LPS challenge

Our data indicate that an acute LPS i.p. challenge was sufficient to rapidly activate both microglia and astrocytes to induce cytokine expression and promote sickness behavior. However, the morphological changes lagged the mRNA activation profile. Other studies have used a repeated LPS injection paradigm (i.e., LPS pre-conditioning) with four injections to investigate microglial activation and neuroprotective properties (Cardona et al., 2006; Chen et al., 2014; Chen et al., 2012). Therefore, we next sought to determine the degree to which an acute LPS injection differed from the repeated LPS injection in the context of sickness behavior, glial cytokine induction, and morphological changes. To be consistent with other studies using repeated LPS injections, a higher dosage of LPS (20 μg per mouse) was used (Bodea et al., 2014; Cardona et al., 2006; Chen et al., 2012; Puntener et al., 2012). This dose was twice as high as the LPS dosage used in Figs.1–3. The diagram provided (Fig.4A) outlines that mice received either one (LPS 1×) or four daily injections (LPS 4×) of LPS (20 μg) and behavior and mRNA/morphological analyses were determined 24 h after the last LPS injection.

The percentage of body weight loss was determined over the 4 days of repeated LPS injections. Mice injected repeatedly with LPS lost body weight ($p<0.01$, Fig.4B). During the course of four daily injections, however, loss of body weight occurred only during the first two days and was maintained during the subsequent two days of LPS injections. Social exploratory behavior was determined at baseline and again 4, 12 and 24 h after the last LPS injection. Similar to the behavioral response induced by 10 μg of LPS (Fig.1D), social exploratory behavior was reduced 4 and 12 h after LPS ($p<0.01$, for each) but was resolved by 24 h after LPS 1× injection (Fig. 4C). In the LPS 4× mice, however, there was no significant reduction in social exploratory behavior 4, 12, or 24 h after the last LPS injection.

To assess the peripheral cytokine response, IL-6 levels were determined in the plasma 24 h after the last injection of LPS. Plasma IL-6 levels were elevated in LPS 1× mice compared to saline controls ($p<0.01$, Fig.4D). Plasma IL-6 levels in LPS 4× mice, however, were decreased and not different from saline controls. Overall, LPS 1× mice had evidence of "active sickness response" 4–12 h later but these differences in behavioral and were no longer evident after the 4th repeated injection of LPS.

A more pronounced active inflammatory response was evident in the brain 24 h after acute LPS challenge compared to repeated LPS challenge

After completion of the behavioral testing (24 h), a coronal brain section was collected to assess the overall inflammatory status of the brain (Fig.5A). In these samples, mRNA expression of several pro-inflammatory (IL-1β and TNFα), regulatory (IL-4Rα, YM-1,

TGFβ), and acute phase genes (Saa3, CerulP, HaptoG) were determined. Fig.5A&B shows that mRNA levels of IL-1β and TNFα were elevated in LPS 1× mice ($p<0.01$) but were attenuated in LPS 4× mice ($p<0.01$). The regulatory gene, IL-4Rα, was also highest in the LPS 1× mice compared to all other groups ($p<0.01$). YM-1 and TGFβ were increased following both one and four injections of LPS ($p<0.01$). Similarly, acute phase genes, Saa3, CerulP, and HaptoG, were increased in the brain 24 h after the last injection of LPS 1× and LPS 4× mice ($p<0.05$, for all).

Next, mRNA expression of two inflammatory mediators (IL-1β and TNFα), two regulatory genes (IL-4Rα and YM-1), and one acute phase gene (HaptoG) were determined in Percoll-enriched microglia. IL-1β mRNA was elevated at 24 h in LPS 1× mice ($p<0.01$) but these IL-1β levels were attenuated in LPS 4× mice ($p=0.06$, Fig.5B). In addition, TNFα was still increased 24 h after LPS 1× ($p<0.03$), but was no longer increased 24 h after the last injection of LPS in LPS 4× mice (Fig.5C). Similarly, Fig.5D shows that IL-4Rα was still elevated 24 h after LPS in LPS 1× mice ($p<0.04$) but these levels were attenuated in LPS 4× mice. YM-1 mRNA levels tended to be increased 24 h after LPS in 1× mice ($p=0.1$), and these levels were further elevated in LPS 4× mice compared to all other treatment groups ($p<0.02$, Fig.5E). The acute phase gene HaptoG was also elevated in both LPS 1× ($p<0.02$) and LPS 4× mice, and these levels were significantly increased in LPS 4× mice compared to all other treatment groups ($p<0.01$, Fig. 5F). Taken together, the expression of pro-inflammatory genes was decreased in microglia from mice with repeated LPS injections while the mRNA expression of YM-1 and HaptoG were enhanced.

Increased Iba-1 immunoreactivity of microglia in the cortex and hippocampus 24 h after acute and repeated LPS challenge with no change of GFAP immunoreactivity of astrocytes

The behavioral data indicate that the LPS 4× mice do not have an active sickness response and the microglia of LPS 4× mice have more of a resolution phase mRNA profile compared to the LPS 1× mice. Next we sought to determine the degree to which morphology differences correlated with the resolution phenotype. The morphological profile of microglia (Fig.6A) and astrocytes (Fig.6B) was assessed 24 h after the last LPS injection. Fig.6A shows representative Iba-1 labeling in the cortex of saline (0 h) and LPS (1×, 4×) injected mice 24 h after the final LPS injection. Microglia of both LPS 1× and LPS 4× mice had larger cell bodies and thicker processes. There was a significant increase in Iba-1 immunoreactivity of microglia following either LPS 1× or LPS 4× injection in both the frontal cortex ($p<0.05$, Fig.6C) and hippocampus ($p<0.05$, Fig.6D) 24 h after the last LPS injection. There was no difference in Iba-1 immunoreactivity of microglia between mice injected one or four days with LPS. Therefore, independent of repeated injection, microglia 24–48 h after LPS had increased Iba-1 immunoreactivity.

Fig.6B shows representative GFAP labeling in the hippocampus of saline (0 h) and LPS (1×, 4×) injected mice 24 h after the last LPS injection. Again, there was no difference in GFAP morphology or immunoreactivity of astrocytes following one or four repeated LPS injections (Fig.6B&E). Overall, these data show that while there were behavioral and mRNA profile differences between one and four repeated LPS injected mice, there were no detectable differences in glial morphology.

Discussion

There is significant interest in understanding the role of glial cells under homeostatic and inflammatory conditions. Emerging evidence indicates that microglia and astrocytes have specific and dynamic roles during immune activation. One issue in glia biology, however, is that morphological analysis alone is used to report on the activation state of microglia and astrocytes. Here we show that elevated cytokine expression by microglia correlates to active sickness behavior and precedes alterations in glial morphology. For example, microglia had increased inflammatory cytokine mRNA expression during the active sickness behavior phase (Fig.7). Increased Iba-l immunoreactivity and morphological alterations in microglia, however, were delayed and were only evident during the resolution/recovery phase. While astrocytes also had increased inflammatory mRNA expression, these were delayed compared to microglia and there was no increase in GFAP immunoreactivity at any time point after LPS. Moreover, cytokine induction in glia also did not correlate with morphological changes after repeated LPS challenge. Taken together, Iba-1 and GFAP labeling alone were unreliable readouts of "glial activation" in the context of LPS-induced sickness behavior. Thus, this study highlights the importance of using a multi-pronged approach to report on activation states of glia.

One important component of this study is that LPS-induced sickness behavior is cytokine (IL-1, IL-6, TNF) mediated, (Bluthe et al., 2000a; Bluthe et al., 2000b; Laye et al., 2000; Skelly et al., 2013) so it provides a functional basis to compare glial mRNA, morphological, and behavioral profiles to each other. Notably, activation of the neurovascular unit (endothelial cells) is a key component to how the induction of a peripheral innate immune response communicates to the brain (Ching et al., 2007; Gosselin and Rivest, 2008; Serrats et al., 2010; Skelly et al., 2013; Wohleb et al., 2014). Once that signal gets to the brain, it is propagated by cytokine production from perivascular macrophages and microglia (Henry et al., 2009; Norden et al., 2014a; Serrats et al., 2010; Zamanian et al., 2012). Thus, this is a complex and highly coordinated interaction between several cell types within the CNS. Here we show that genes associated with M1 (IL-1β, TNFα, IL-6), M2 (IL-10, IL-4Rα, YM-1) and acute phase (Saa3, CerulP, HaptoG) responses were increased following LPS injection in coronal brain sections. Consistent with previous studies, M2 markers IL-4Rα and IL-10 were significantly increased concomitant with the induction of pro-inflammatory markers during active sickness behavior 2–4 h (Fenn et al., 2012; Henry et al., 2009; Sierra et al., 2007). There was not a clear shift from M1 to M2 profile with the resolution of LPS-induced sickness behavior. Nonetheless, there was a time dependent transition from an active to a resolution phase of glial activation, which is outlined in Fig.7. For example, there was a persistence of regulatory factors including IL-10, YM-1 and HaptoG in microglia and TGFβ in astrocytes during the resolution phase. Despite these data, understanding differences in M1 and M2 activation profiles of microglia is relevant in neurotrauma, aging, and disease (Cunningham, 2013; Kumar et al., 2013; Norden et al., 2014b). For instance, an enhanced M1 profile of microglia with age or after TBI was detrimental to recovery from LPS challenge and was associated with exaggerated microglial activation and prolonged sickness and depressive-like behaviors (Fenn et al., 2014a; Godbout et al., 2005; Godbout et al., 2008; Wynne et al., 2010). In addition, a reduced M2 profile of microglia and macrophages

after TBI or SCI was associated with more tissue damage and reduced functional recovery in aged rodents (Fenn et al., 2014b; Kumar et al., 2013). Overall, we show that active sickness behavior after LPS was associated with parallel induction of M1 and M2 related genes.

Our data also show the direct association between microglial specific expression of pro-inflammatory cytokines and the induction and maintenance of sickness behavior. As expected, LPS i.p. injection (10 or 20 μg) elicited a transient sickness behavioral response evident within 2 h and resolved by 24 h (Berg et al., 2004). Sickness behavior at the acute time points (2–4 h) corresponded with robust pro-inflammatory cytokine (IL-1β, TNFα) expression specifically by microglia (and not astrocytes). Notably, significant microglial depletion with CSF1R antagonist attenuated LPS-induced IL-1β and TNFα expression in the brain (Elmore et al., 2014). These data are consistent with a study using minocycline, a purported microglia inhibitor, which reduced microglia, attenuated IL-1 and TNF expression, and facilitated the recovery from LPS induced sickness behavior (Henry et al., 2008). Although mRNA expression was determined in this study, we have previously detected correspondingly higher protein levels of IL-1β and IL-4Rα in microglia 4 h after LPS (Henry et al., 2009)(Fenn et al., 2012). In addition, we have reported a robust reduction of CX_3CR1 (fractalkine receptor) on the surface of microglia at 4 h after LPS (Wynne et al., 2010). Furthermore, CX_3CR1 surface expression on microglia of adult mice returned to baseline at 24 h, parallel with resolution of pro-inflammatory cytokine expression and the recovery from sickness behavior (Wynne et al., 2010). Overall, the timing of microglial pro-inflammatory cytokine expression reflects active sickness behavior induced by LPS challenge.

Novel data also shows that the peak of inflammatory cytokine expression by astrocytes (IL-1β, CCL2, TNFα) occurred 12 h after LPS. Notably this induction of CCL2 and TNFα was delayed compared to the rapid and robust cytokine induction by microglia. These data are interpreted to indicate sequential glia activation with microglia becoming activated first, and then astrocytes are activated. It is unclear, however, if this sequential cytokine induction by astrocytes 12–24 h after LPS represents an inflammatory or regulatory response. For example, the timing of the astrocyte peak expression of cytokine mRNA corresponds with the resolution of sickness behavior and microglial activation. Moreover, this secondary activation of astrocytes was associated with higher TGFβ mRNA induction. This is relevant because our previous work indicates that IL-10 produced by microglia stimulates astrocytic TFGβ, which provides negative feedback on microglial activation and attenuates sickness behavior (Norden et al., 2014a). Here, delayed induction of TGFβ mRNA was detected in astrocytes, but no relative induction in microglia. Also consistent with our previous study, microglia had strong induction of IL-10 after LPS, but IL-10 was not increased in astrocytes. Overall, there is key differential expression and timing of cytokine expression of microglia and astrocytes that are interpreted to indicate sequential activation and evidence of dynamic communication between two cell types.

Another relevant aspect of this study is the lack of connection between the morphological profile of glia and the corresponding increased inflammatory mRNA profile after LPS challenge. Importantly, neither behavior nor mRNA profiles of microglia corresponded with the increased de-ramified Iba-1 morphology of microglia. During the active cytokine

expression phase 2–12 h after LPS, microglia from saline and LPS injected mice displayed similar Iba-1 immunoreactivity. Increased Iba-1 immunoreactivity and de-ramification was not detected in the hippocampus and cortex until 24–48 h after LPS. On an mRNA level, Iba-1 expression also had a delayed induction following LPS (24–48 h). These data are consistent with a previous study using LPS injection in a model of preclinical prion disease where differential cytokine induction was detected independent of morphological differences (Cunningham et al., 2005b). Similar to the microglial assessments, astrocytes had an increased mRNA expression profile associated with activation but did not have a corresponding increase in GFAP immunoreactivity. Furthermore, incongruence between the activation mRNA profile of glia and morphological changes was also evident in the repeated LPS challenge. LPS (10 μg), LPS (20 μg), and LPS 4× (20 μg) all had different mRNA profiles but the same level of Iba-1 and GFAP immunoreactivity 24 h after the last LPS injection. Thus, morphological analysis alone would not provide a representative assessment of activation following acute or repeated LPS challenge. Our collective data indicate that the de-ramified morphology after a peripheral challenge with LPS represents a resolution phase of microglia cytokine induction and corresponding sickness behavior.

Our study highlights the limitations of myriad studies that only use Iba-1 and GFAP labeling and report on the "inflammatory" states of glia. Indeed, the data from our time course provided in this study show the importance of using multiple approaches (behavior, glial specific mRNA, morphology) when reporting on the level of microglial activation. We acknowledge that when microglia are chronically activated in neurodegenerative disease (Cameron et al., 2012; Cunningham et al., 2005a), CNS infection (Nayak et al., 2013), traumatic CNS injury (Cao et al., 2012; Detloff et al., 2008; Kumar et al., 2013), or stress (Kreisel et al., 2014; Wohleb et al., 2011) a de-ramified Iba-1 profile of microglia is likely a good representation of a pro-inflammatory profile. In addition, other more sensitive morphological approaches that include analysis of glial soma area, cell length, cell perimeter, process length and size may be more revealing about activation state (Kongsui et al., 2014). Although, based on how rapidly active microglia express cytokines, there will be a significant time lag between activation and the detection of any of these morphological differences.

Another important finding is that repeated LPS injections did not amplify the response to LPS in the context of sickness behavior and biochemical or morphological analysis of glia. Four repeated injections of LPS (provided every 24 h) led to immune tolerance and an overall less inflammatory profile in the brain compared to 24 h after an acute injection of the same LPS dose. In support of this idea, LPS 4× mice showed no sickness behavior 24 h after the last injection. In addition, plasma IL-6 levels were no longer elevated 24 h after the fourth injection of LPS. These data are consistent with studies showing that multiple exposures to the same stimuli lead to immune tolerance of peritoneal macrophages (Biswas and Lopez-Collazo, 2009), which are the cells responding to the i.p injection of LPS. Notably, LPS 1× and LPS 4× mice had a similar de-ramified morphology of microglia. Enriched microglia from LPS 4× mice, however, had lower inflammatory cytokine mRNA expression and maintained higher levels of YM-1 (M2) and HaptoG (acute phase) expression compared to microglia from LPS 1× mice. It is important to mention that the amplified YM-1 mRNA induction in microglia in LPS 4× mice compared to LPS 1× mice

was not reflected in the coronal brain section. Thus, YM-1 was specifically upregulated in enriched microglia. Overall, this anti-inflammatory profile of microglia associated with repeated LPS challenges is proposed to be neuroprotective (Chen et al., 2014). For example, repeated LPS injection prior to brain injury was associated with reduced cell death and lesion volume induced by cryogenic brain injury (Chen et al., 2012). Similar to our data, at 24 h after the last injection of LPS, microglia had pronounced de-ramified morphology, higher YM-1 and IL-4Rα, and a lower M1 profile (Chen et al., 2012). This increased microglial expression of YM-1 is important as it represents an enhanced M2a and repair supportive profile (Colton, 2009). Similar to repeated LPS injections, YM-1 expression was also enhanced in microglia by the anti-inflammatory agent minocycline (Fenn et al., 2012) and by IL-4 administration (Pepe et al., 2014). The maintenance of elevated HaptoG expression in microglia may represent a profile consistent with neuroprotection and iron sequestration following CNS injury (Zhao et al., 2009). Overall, repeated injections of LPS did not amplify the inflammatory response, however, it may shift the microglia profile towards neuroprotection.

The data collected in this repeated LPS paradigm was during the resolution phase of microglial activation (24 h). Thus, the potential neuroprotective properties of microglia after inflammatory resolution are likely time dependent and not solely an effect of repeated LPS injections. In fact, studies have also reported less extensive injury when pre-treated with acute LPS 24–72 h prior to CNS injury (Hayakawa et al., 2014; Stevens et al., 2011). At the height of inflammation, however, the potential of microglia to be neuroprotective may be altered. For instance, cytokine levels in the brain were elevated after 2 injections of LPS compared to 1 injection at an acute time point after LPS (3 h) (Puntener et al., 2012). While we report on repeated injections being immune tolerant, another study showed that microglia were more activated following four repeated injections of LPS (1μg/gbw) compared to one injection (4μg/gbw) (Bodea et al., 2014). In this study, however, microglia were analyzed by Iba-1 immunoreactivity 4 days after the single injection and only 24 h after the 4th repeated injection. Overall, our study is consistent with the notion that the resolution phase of microglial activation, independent of acute or repeated LPS challenge, is potentially neuroprotective.

In summary, neither Iba-1 nor GFAP immunoreactivity alone adequately informed on the pro-inflammatory state of microglia or astrocytes. In the context of a peripheral LPS challenge, Iba-1 immunoreactivity 24–48 h after LPS corresponded with the resolution phase of the cytokine and behavioral response. We also provide evidence of a delayed response of astrocytes that may correspond with anti-inflammatory feedback on microglia. In addition, mice with repeated LPS injections had a similar morphological profile of microglia as acute LPS injected mice but had reduced inflammatory mRNA profile and attenuated sickness behavior. Collectively, these data indicate that multiple approaches (behavior, glial specific mRNA, and morphology) are required to provide a reliable interpretation of the inflammatory profile and the activation state of glia.

Acknowledgements

References

Berg BM, Godbout JP, Kelley KW, Johnson RW. Alpha-tocopherol attenuates lipopolysaccharide-induced sickness behavior in mice. Brain, behavior, and immunity. 2004; 18:149–157.

Biber K, Neumann H, Inoue K, Boddeke HW. Neuronal 'On' and 'Off' signals control microglia. Trends in neurosciences. 2007; 30:596–602. [PubMed: 17950926]

Biswas SK, Lopez-Collazo E. Endotoxin tolerance: new mechanisms, molecules and clinical significance. Trends in immunology. 2009; 30:475–487. [PubMed: 19781994]

Bluthe RM, Laye S, Michaud B, Combe C, Dantzer R, Parnet P. Role of interleukin-1beta and tumour necrosis factor-alpha in lipopolysaccharide-induced sickness behaviour: a study with interleukin-1 type I receptor-deficient mice. The European journal of neuroscience. 2000a; 12:4447–4456. [PubMed: 11122355]

Bluthe RM, Michaud B, Poli V, Dantzer R. Role of IL-6 in cytokine-induced sickness behavior: a study with IL-6 deficient mice. Physiology & behavior. 2000b; 70:367–373. [PubMed: 11006436]

Bodea LG, Wang Y, Linnartz-Gerlach B, Kopatz J, Sinkkonen L, Musgrove R, Kaoma T, Muller A, Vallar L, Di Monte DA, Balling R, Neumann H. Neurodegeneration by activation of the microglial complement-phagosome pathway. The Journal of neuroscience. 2014; 34:8546–8556. [PubMed: 24948809]

Cameron B, Tse W, Lamb R, Li X, Lamb BT, Landreth GE. Loss of interleukin receptor-associated kinase 4 signaling suppresses amyloid pathology and alters microglial phenotype in a mouse model of Alzheimer's disease. The Journal of neuroscience. 2012; 32:15112–15123. [PubMed: 23100432]

Cao T, Thomas TC, Ziebell JM, Pauly JR, Lifshitz J. Morphological and genetic activation of microglia after diffuse traumatic brain injury in the rat. Neuroscience. 2012; 225:65–75. [PubMed: 22960311]

Cardona AE, Pioro EP, Sasse ME, Kostenko V, Cardona SM, Dijkstra IM, Huang D, Kidd G, Dombrowski S, Dutta R, Lee JC, Cook DN, Jung S, Lira SA, Littman DR, Ransohoff RM. Control of microglial neurotoxicity by the fractalkine receptor. Nature neuroscience. 2006; 9:917–924. [PubMed: 16732273]

Carpentier PA, Begolka WS, Olson JK, Elhofy A, Karpus WJ, Miller SD. Differential activation of astrocytes by innate and adaptive immune stimuli. Glia. 2005; 49:360–374. [PubMed: 15538753]

Carson MJ, Doose JM, Melchior B, Schmid CD, Ploix CC. CNS immune privilege: hiding in plain sight. Immunol Rev. 2006; 213:48–65. [PubMed: 16972896]

Cazareth J, Guyon A, Heurteaux C, Chabry J, Petit-Paitel A. Molecular and cellular neuroinflammatory status of mouse brain after systemic lipopolysaccharide challenge: importance of CCR2/CCL2 signaling. Journal of neuroinflammation. 2014; 11:132. [PubMed: 25065370]

Chen Z, Jalabi W, Hu W, Park HJ, Gale JT, Kidd GJ, Bernatowicz R, Gossman ZC, Chen JT, Dutta R, Trapp BD. Microglial displacement of inhibitory synapses provides neuroprotection in the adult brain. Nature communications. 2014; 5:4486.

Chen Z, Jalabi W, Shpargel KB, Farabaugh KT, Dutta R, Yin X, Kidd GJ, Bergmann CC, Stohlman SA, Trapp BD. Lipopolysaccharide-induced microglial activation and neuroprotection against experimental brain injury is independent of hematogenous TLR4. The Journal of neuroscience. 2012; 32:11706–11715. [PubMed: 22915113]

Ching S, Zhang H, Belevych N, He L, Lai W, Pu XA, Jaeger LB, Chen Q, Quan N. Endothelial-specific knockdown of interleukin-1 (IL-1) type 1 receptor differentially alters CNS responses to IL-1 depending on its route of administration. The Journal of neuroscience. 2007; 27:10476–10486. [PubMed: 17898219]

Author Manuscript Author Manuscript Author Manuscript Author Manuscript

Colton CA. Heterogeneity of microglial activation in the innate immune response in the brain. Journal of neuroimmune pharmacology. 2009; 4:399–418. [PubMed: 19655259]

Cunningham C. Microglia and neurodegeneration: the role of systemic inflammation. Glia. 2013; 61:71–90. [PubMed: 22674585]

Cunningham C, Wilcockson DC, Boche D, Perry VH. Comparison of inflammatory and acute-phase responses in the brain and peripheral organs of the ME7 model of prion disease. J Virol. 2005a; 79:5174–5184. [PubMed: 15795301]

Cunningham C, Wilcockson DC, Campion S, Lunnon K, Perry VH. Central and systemic endotoxin challenges exacerbate the local inflammatory response and increase neuronal death during chronic neurodegeneration. The Journal of neuroscience. 2005b; 25:9275–9284. [PubMed: 16207887]

Dantzer R. Cytokine-induced sickness behavior: mechanisms and implications. Annals of the New York Academy of Sciences. 2001; 933:222–234. [PubMed: 12000023]

Dantzer R, O'Connor JC, Freund GG, Johnson RW, Kelley KW. From inflammation to sickness and depression: when the immune system subjugates the brain. Nature reviews. Neuroscience. 2008; 9:46–56. [PubMed: 18073775]

Davalos D, Grutzendler J, Yang G, Kim JV, Zuo Y, Jung S, Littman DR, Dustin ML, Gan WB. ATP mediates rapid microglial response to local brain injury in vivo. Nature neuroscience. 2005; 8:752–758. [PubMed: 15895084]

Detloff MR, Fisher LC, McGaughy V, Longbrake EE, Popovich PG, Basso DM. Remote activation of microglia and pro-inflammatory cytokines predict the onset and severity of below-level neuropathic pain after spinal cord injury in rats. Experimental neurology. 2008; 212:337–347. [PubMed: 18511041]

Donnelly DJ, Gensel JC, Ankeny DP, van Rooijen N, Popovich PG. An efficient and reproducible method for quantifying macrophages in different experimental models of central nervous system pathology. J Neurosci Methods. 2009; 181:36–44. [PubMed: 19393692]

Elmore MR, Najafi AR, Koike MA, Dagher NN, Spangenberg EE, Rice RA, Kitazawa M, Matusow B, Nguyen H, West BL, Green KN. Colony-stimulating factor 1 receptor signaling is necessary for microglia viability, unmasking a microglia progenitor cell in the adult brain. Neuron. 2014; 82:380–397. [PubMed: 24742461]

Farina C, Aloisi F, Meinl E. Astrocytes are active players in cerebral innate immunity. Trends in immunology. 2007; 28:138–145. [PubMed: 17276138]

Fenn AM, Gensel JC, Huang Y, Popovich PG, Lifshitz J, Godbout JP. Immune activation promotes depression 1 month after diffuse brain injury: a role for primed microglia. Biol Psychiatry. 2014a; 76:575–584. [PubMed: 24289885]

Fenn AM, Hall JC, Gensel JC, Popovich PG, Godbout JP. IL-4 Signaling Drives a Unique Arginase+/IL-1beta+ Microglia Phenotype and Recruits Macrophages to the Inflammatory CNS: Consequences of Age-Related Deficits in IL-4Ralpha after Traumatic Spinal Cord Injury. The Journal of neuroscience. 2014b; 34:8904–8917. [PubMed: 24966389]

Fenn AM, Henry CJ, Huang Y, Dugan A, Godbout JP. Lipopolysaccharide-induced interleukin (IL)-4 receptor-alpha expression and corresponding sensitivity to the M2 promoting effects of IL-4 are impaired in microglia of aged mice. Brain, behavior, and immunity. 2012; 26:766–777.

Godbout JP, Chen J, Abraham J, Richwine AF, Berg BM, Kelley KW, Johnson RW. Exaggerated neuroinflammation and sickness behavior in aged mice following activation of the peripheral innate immune system. FASEB journal. 2005; 19:1329–1331. [PubMed: 15919760]

Godbout JP, Moreau M, Lestage J, Chen J, Sparkman NL, J OC, Castanon N, Kelley KW, Dantzer R, Johnson RW. Aging exacerbates depressive-like behavior in mice in response to activation of the peripheral innate immune system. Neuropsychopharmacology. 2008; 33:2341–2351. [PubMed: 18075491]

Gosselin D, Rivest S. MyD88 signaling in brain endothelial cells is essential for the neuronal activity and glucocorticoid release during systemic inflammation. Molecular psychiatry. 2008; 13:480–497. [PubMed: 18180766]

Hansen MK, O'Connor KA, Goehler LE, Watkins LR, Maier SF. The contribution of the vagus nerve in interleukin-1beta-induced fever is dependent on dose. American journal of physiology. Regulatory, integrative and comparative physiology. 2001; 280:R929–R934.

Hayakawa K, Okazaki R, Morioka K, Nakamura K, Tanaka S, Ogata T. Lipopolysaccharide preconditioning facilitates M2 activation of resident microglia after spinal cord injury. Journal of neuroscience research. 2014; 92:1647–1658. [PubMed: 25044014]

Henry CJ, Huang Y, Wynne A, Hanke M, Himler J, Bailey MT, Sheridan JF, Godbout JP. Minocycline attenuates lipopolysaccharide (LPS)-induced neuroinflammation, sickness behavior, and anhedonia. Journal of neuroinflammation. 2008; 5:15. [PubMed: 18477398]

Henry CJ, Huang Y, Wynne AM, Godbout JP. Peripheral lipopolysaccharide (LPS) challenge promotes microglial hyperactivity in aged mice that is associated with exaggerated induction of both pro-inflammatory IL-1beta and anti-inflammatory IL-10 cytokines. Brain, behavior, and immunity. 2009; 23:309–317.

John GR, Chen L, Rivieccio MA, Melendez-Vasquez CV, Hartley A, Brosnan CF. Interleukin-1beta induces a reactive astroglial phenotype via deactivation of the Rho GTPase-Rock axis. The Journal of neuroscience. 2004; 24:2837–2845. [PubMed: 15028778]

Kongsui R, Beynon SB, Johnson SJ, Walker FR. Quantitative assessment of microglial morphology and density reveals remarkable consistency in the distribution and morphology of cells within the healthy prefrontal cortex of the rat. Journal of neuroinflammation. 2014; 11:182. [PubMed: 25343964]

Kreisel T, Frank MG, Licht T, Reshef R, Ben-Menachem-Zidon O, Baratta MV, Maier SF, Yirmiya R. Dynamic microglial alterations underlie stress-induced depressive-like behavior and suppressed neurogenesis. Molecular psychiatry. 2014; 19:699–709. [PubMed: 24342992]

Kumar A, Stoica BA, Sabirzhanov B, Burns MP, Faden AI, Loane DJ. Traumatic brain injury in aged animals increases lesion size and chronically alters microglial/macrophage classical and alternative activation states. Neurobiology of aging. 2013; 34:1397–1411. [PubMed: 23273602]

Lacroix S, Feinstein D, Rivest S. The bacterial endotoxin lipopolysaccharide has the ability to target the brain in upregulating its membrane CD14 receptor within specific cellular populations. Brain pathology. 1998; 8:625–640. [PubMed: 9804372]

Laflamme N, Lacroix S, Rivest S. An essential role of interleukin-1beta in mediating NF-kappaB activity and COX-2 transcription in cells of the blood-brain barrier in response to a systemic and localized inflammation but not during endotoxemia. The Journal of neuroscience. 1999; 19:10923–10930. [PubMed: 10594073]

Laye S, Gheusi G, Cremona S, Combe C, Kelley K, Dantzer R, Parnet P. Endogenous brain IL-1 mediates LPS-induced anorexia and hypothalamic cytokine expression. American journal of physiology. Regulatory, integrative and comparative physiology. 2000; 279:R93–R98.

Liu W, Tang Y, Feng J. Cross talk between activation of microglia and astrocytes in pathological conditions in the central nervous system. Life sciences. 2011; 89:141–146. [PubMed: 21684291]

Min KJ, Yang MS, Kim SU, Jou I, Joe EH. Astrocytes induce hemeoxygenase-1 expression in microglia: a feasible mechanism for preventing excessive brain inflammation. The Journal of neuroscience. 2006; 26:1880–1887. [PubMed: 16467537]

Mosser DM, Edwards JP. Exploring the full spectrum of macrophage activation. Nature reviews. Immunology. 2008; 8:958–969. [PubMed: 19029990]

Myer DJ, Gurkoff GG, Lee SM, Hovda DA, Sofroniew MV. Essential protective roles of reactive astrocytes in traumatic brain injury. Brain. 2006; 129:2761–2772. [PubMed: 16825202]

Nayak D, Johnson KR, Heydari S, Roth TL, Zinselmeyer BH, McGavern DB. Type I interferon programs innate myeloid dynamics and gene expression in the virally infected nervous system. PLoS pathogens. 2013; 9:e1003395. [PubMed: 23737750]

Norden DM, Fenn AM, Dugan A, Godbout JP. TGFbeta produced by IL-10 redirected astrocytes attenuates microglial activation. Glia. 2014a; 62:881–895. [PubMed: 24616125]

Norden DM, Godbout JP. Review: microglia of the aged brain: primed to be activated and resistant to regulation. Neuropathology and applied neurobiology. 2013; 39:19–34. [PubMed: 23039106]

Norden DM, Muccigrosso MM, Godbout JP. Microglial Priming and Enhanced Reactivity to Secondary Insult in Aging, and Traumatic CNS injury, and Neurodegenerative Disease. Neuropharmacology. 2014b; 96:29–41. [PubMed: 25445485]

Parrow NL, Fleming RE, Minnick MF. Sequestration and scavenging of iron in infection. Infection and immunity. 2013; 81:3503–3514. [PubMed: 23836822]

Paxinos G, Franklin K. The mouse brain in stereotaxic coordinates (2nd edition). 2004

Puntambekar SS, Davis DS, Hawel L 3rd, Crane J, Byus CV, Carson MJ. LPS-induced CCL2 expression and macrophage influx into the murine central nervous system is polyamine-dependent. Brain, behavior, and immunity. 2011; 25:629–639.

Puntener U, Booth SG, Perry VH, Teeling JL. Long-term impact of systemic bacterial infection on the cerebral vasculature and microglia. Journal of neuroinflammation. 2012; 9:146. [PubMed: 22738332]

Rivest S. Regulation of innate immune responses in the brain. Nature reviews. Immunology. 2009; 9:429–439. [PubMed: 19461673]

Sauerbeck A, Schonberg DL, Laws JL, McTigue DM. Systemic iron chelation results in limited functional and histological recovery after traumatic spinal cord injury in rats. Experimental neurology. 2013; 248:53–61. [PubMed: 23712107]

Sawicki CM, McKim D, Wohleb ES, Jarrett BL, Norden DM, Godbout JP, Sheridan JF. Social defeat promotes a reactive endothelium in a brain region-dependent manner with increased expression of key adhesion molecules, selectins and chemokines associated with the recruitment of myeloid cells to the brain. Journal of Neuroscience. 2014

Serrats J, Schiltz JC, Garcia-Bueno B, van Rooijen N, Reyes TM, Sawchenko PE. Dual roles for perivascular macrophages in immune-to-brain signaling. Neuron. 2010; 65:94–106. [PubMed: 20152116]

Sierra A, Gottfried-Blackmore AC, McEwen BS, Bulloch K. Microglia derived from aging mice exhibit an altered inflammatory profile. Glia. 2007; 55:412–424. [PubMed: 17203473]

Skelly DT, Hennessy E, Dansereau MA, Cunningham C. A systematic analysis of the peripheral and CNS effects of systemic LPS, IL-1beta, [corrected] TNF-alpha and IL-6 challenges in C57BL/6 mice. PloS one. 2013; 8:e69123. [PubMed: 23840908]

Sofroniew MV. Reactive astrocytes in neural repair and protection. The Neuroscientist : a review journal bringing neurobiology, neurology and psychiatry. 2005; 11:400–407.

Stevens SL, Leung PY, Vartanian KB, Gopalan B, Yang T, Simon RP, Stenzel-Poore MP. Multiple preconditioning paradigms converge on interferon regulatory factor-dependent signaling to promote tolerance to ischemic brain injury. The Journal of neuroscience. 2011; 31:8456–8463. [PubMed: 21653850]

Voskuhl RR, Peterson RS, Song B, Ao Y, Morales LB, Tiwari-Woodruff S, Sofroniew MV. Reactive astrocytes form scar-like perivascular barriers to leukocytes during adaptive immune inflammation of the CNS. The Journal of neuroscience. 2009; 29:11511–11522. [PubMed: 19759299]

Wohleb ES, Fenn AM, Pacenta AM, Powell ND, Sheridan JF, Godbout JP. Peripheral innate immune challenge exaggerated microglia activation, increased the number of inflammatory CNS macrophages, and prolonged social withdrawal in socially defeated mice. Psychoneuroendocrinology. 2012; 37:1491–1505. [PubMed: 22386198]

Wohleb ES, Hanke ML, Corona AW, Powell ND, Stiner LM, Bailey MT, Nelson RJ, Godbout JP, Sheridan JF. beta-Adrenergic receptor antagonism prevents anxiety-like behavior and microglial reactivity induced by repeated social defeat. The Journal of neuroscience. 2011; 31:6277–6288. [PubMed: 21525267]

Wohleb ES, Patterson JM, Sharma V, Quan N, Godbout JP, Sheridan JF. Knockdown of interleukin-1 receptor type-1 on endothelial cells attenuated stress-induced neuroinflammation and prevented anxiety-like behavior. The Journal of neuroscience. 2014; 34:2583–2591. [PubMed: 24523548]

Wohleb ES, Powell ND, Godbout JP, Sheridan JF. Stress-induced recruitment of bone marrow-derived monocytes to the brain promotes anxiety-like behavior. The Journal of neuroscience. 2013; 33:13820–13833. [PubMed: 23966702]

Wynne AM, Henry CJ, Huang Y, Cleland A, Godbout JP. Protracted downregulation of CX(3)CR1 on microglia of aged mice after lipopolysaccharide challenge. Brain, behavior, and immunity. 2010; 24:1190–1201.

Zamanian JL, Xu L, Foo LC, Nouri N, Zhou L, Giffard RG, Barres BA. Genomic analysis of reactive astrogliosis. The Journal of neuroscience. 2012; 32:6391–6410. [PubMed: 22553043]

Zhang Y, Barres BA. Astrocyte heterogeneity: an underappreciated topic in neurobiology. Current opinion in neurobiology. 2010; 20:588–594. [PubMed: 20655735]

Zhao X, Song S, Sun G, Strong R, Zhang J, Grotta JC, Aronowski J. Neuroprotective role of haptoglobin after intracerebral hemorrhage. The Journal of neuroscience. 2009; 29:15819–15827. [PubMed: 20016097]

## Main points

Increased pro-inflammatory cytokine expression by microglia correlated with active sickness behavior. Increased morphological activation was delayed following the LPS injection and corresponded with a resolution phase of microglia activation. Microglial Iba-1 or astrocytic GFAP immunoreactivity are unreliable indicators of activation and a multipronged approach is necessary to report on the activation state of glia.
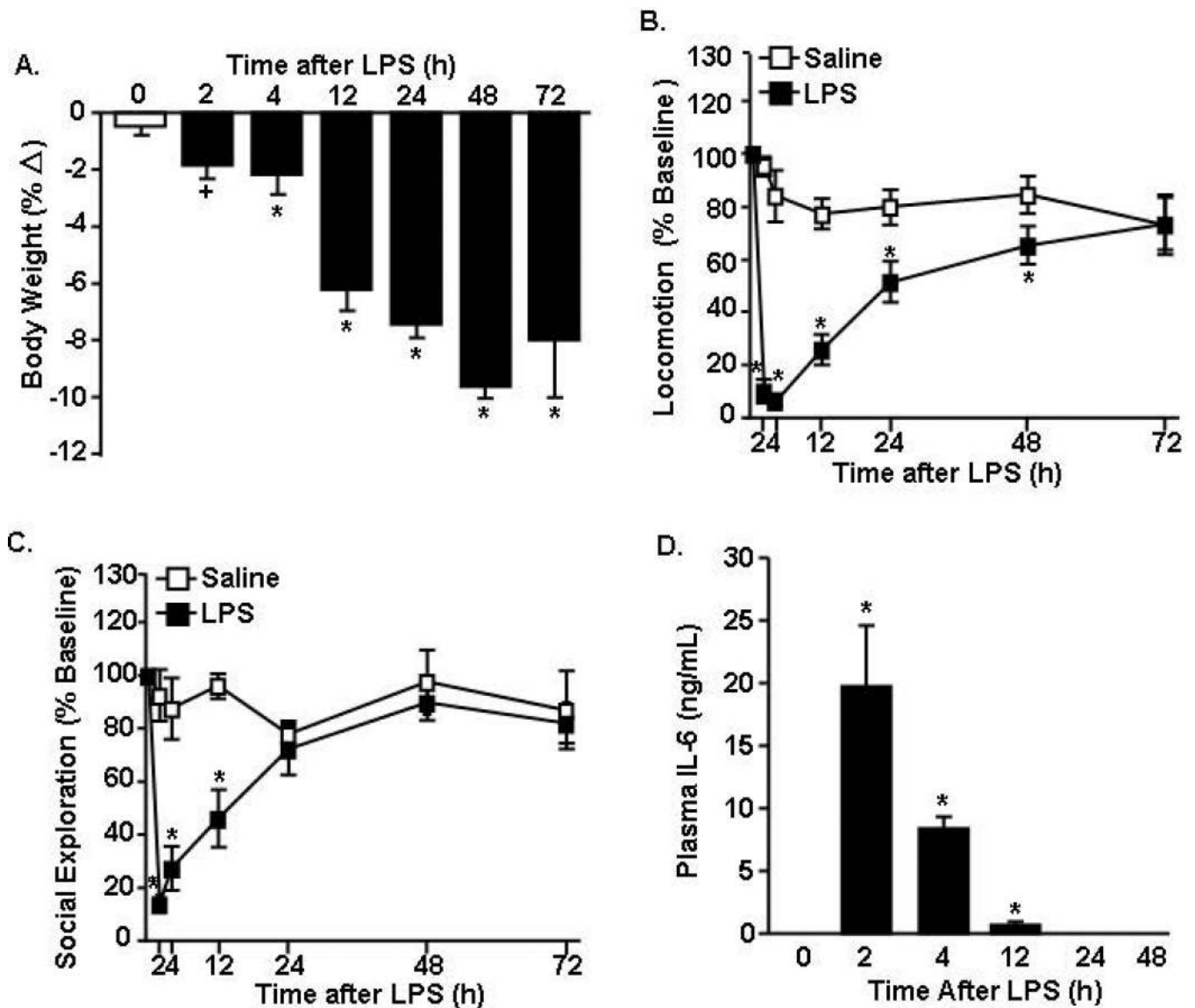
Figure 1. Acute LPS challenge promoted a transient sickness response that was resolved within 48 h

Adult BALB/c mice were injected (i.p.) with saline or LPS (10 μg). Over a 72 h time course, A) body weight, B) locomotor activity, and C) social exploratory behavior were determined. D) IL-6 protein levels were determined in plasma collected 2, 4, 12, 24, and 48 h later. Data expressed as percent change from baseline. Means with (*) are different from saline controls ($p<0.05$) and means with (+) tend to be different from saline controls ($p=0.06$–0.10).
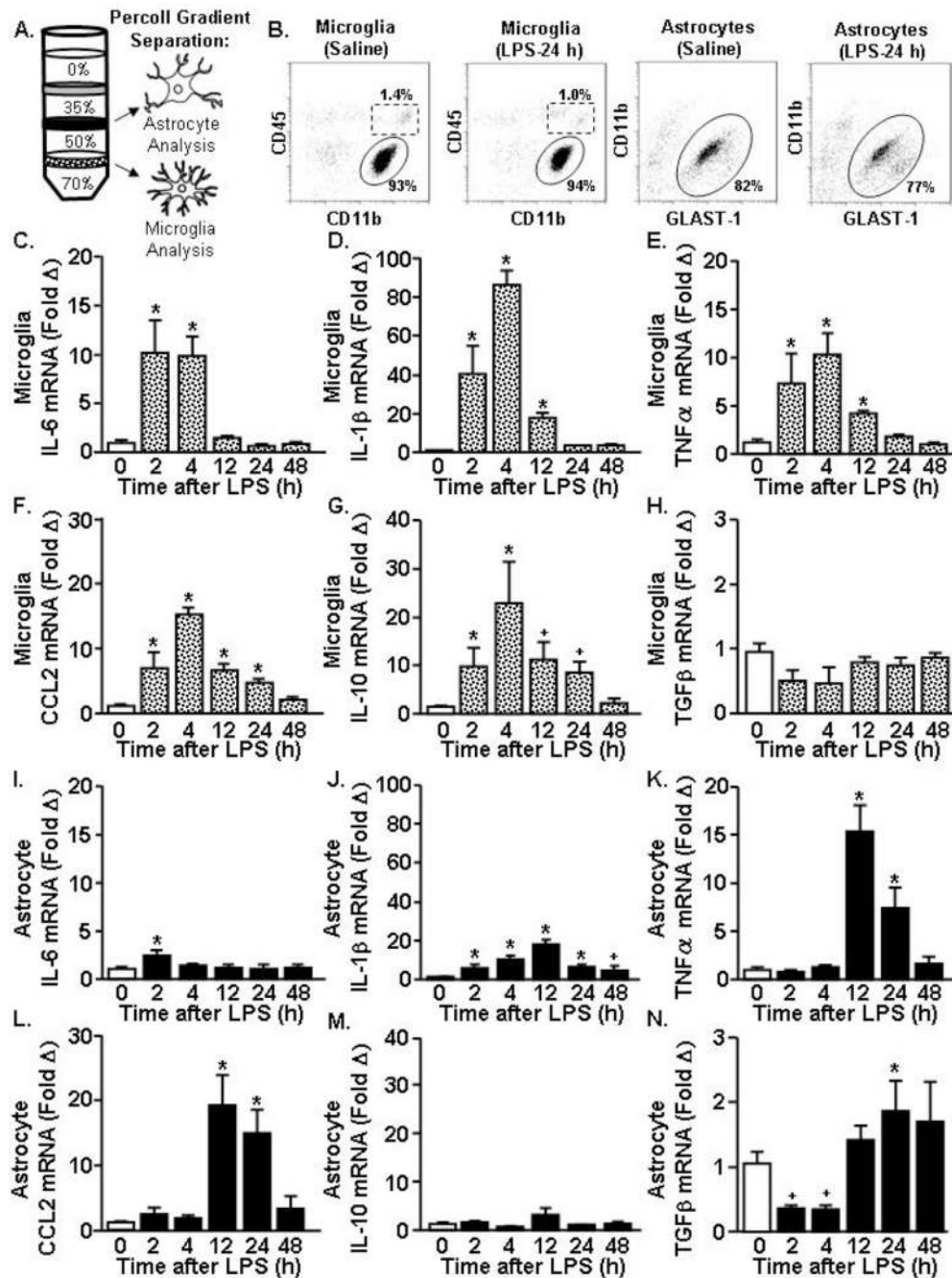
Figure 2. Rapid microglial cytokine induction after acute LPS challenge preceded astrocyte cytokine expression

Adult mice received (i.p.) saline or LPS (10 μg) and A) astrocytes and microglia were isolated and Percoll-enriched 2, 4, 12, 24, and 48 h later. B) Representative bivariate dot plots of CD11b and CD45 labeling of microglia and CD11b and Glast-1 labeling of astrocytes collected after Percoll enrichment. Levels of C) IL-6, D) IL-1β, E) TNFα, F) CCL2, G) IL-10, and H) TGFβ mRNA were determined in enriched microglia. The expression levels for I) IL-6, J) IL-1β, K) TNFα, L) CCL2, M) IL-10, and N) TGFβ were

determined in enriched astrocytes. Means with (*) are different from saline controls ($p<0.05$) and means with (+) tend to be different from saline controls ($p=0.06–0.10$).
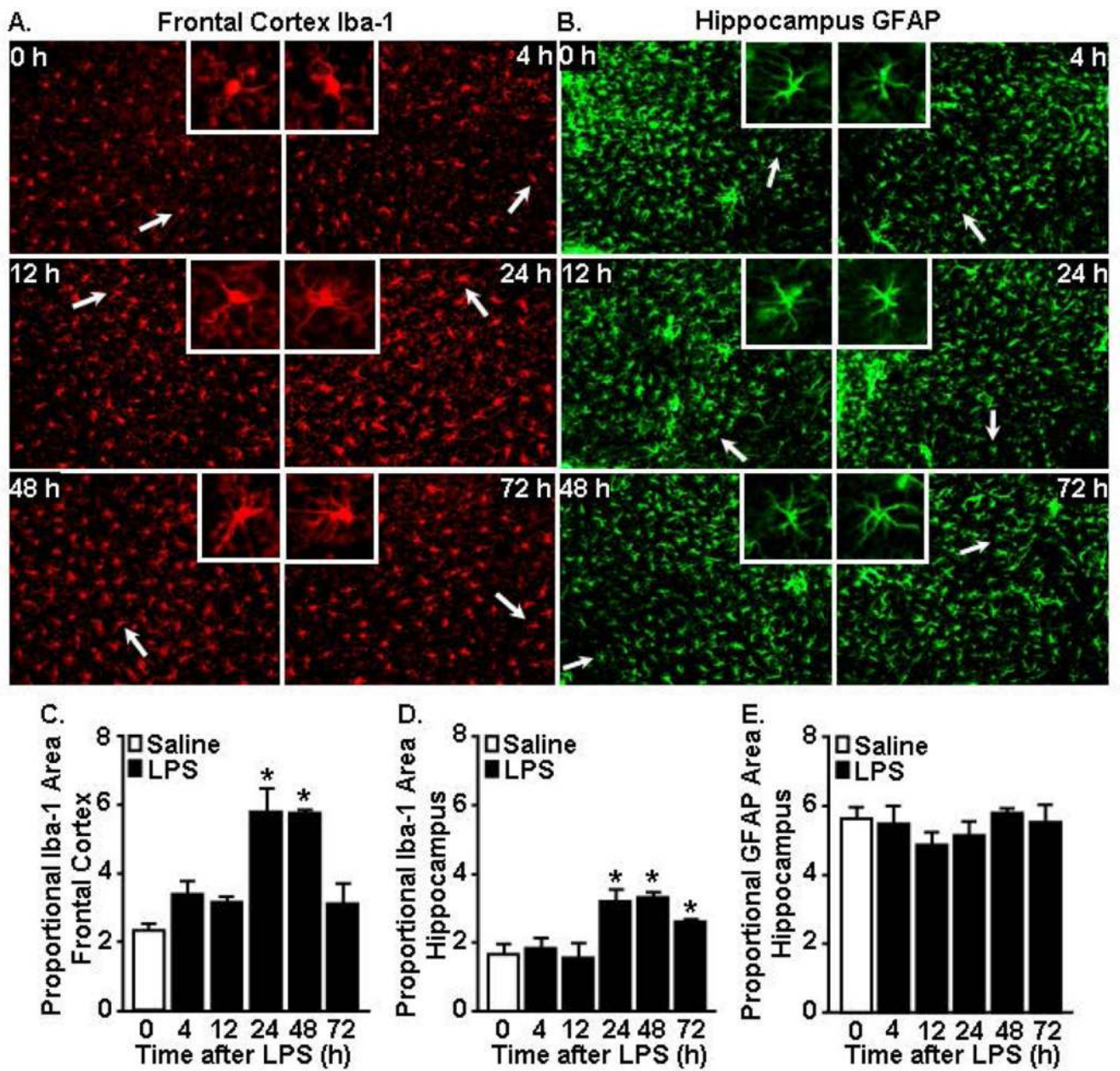
Figure 3. Iba-1 immunoreactivity of microglia increased 24 and 48 h after acute LPS challenge while GFAP immunoreactivity of astrocytes was unaffected

Brains were collected and Iba-1 and GFAP immunoreactivity was determined 4, 12, 24, 48, and 72 h after saline or LPS (10 μg) injection. Representative images of labeling for A) Iba-1 (cortex) and B) GFAP (hippocampus) are shown. White arrows indicate the enlarged insert of a representative cell. Proportional area of Iba-1 in the C) frontal cortex and D) hippocampus. E) Proportional area of GFAP in the hippocampus. $^*p < 0.05$ from saline.
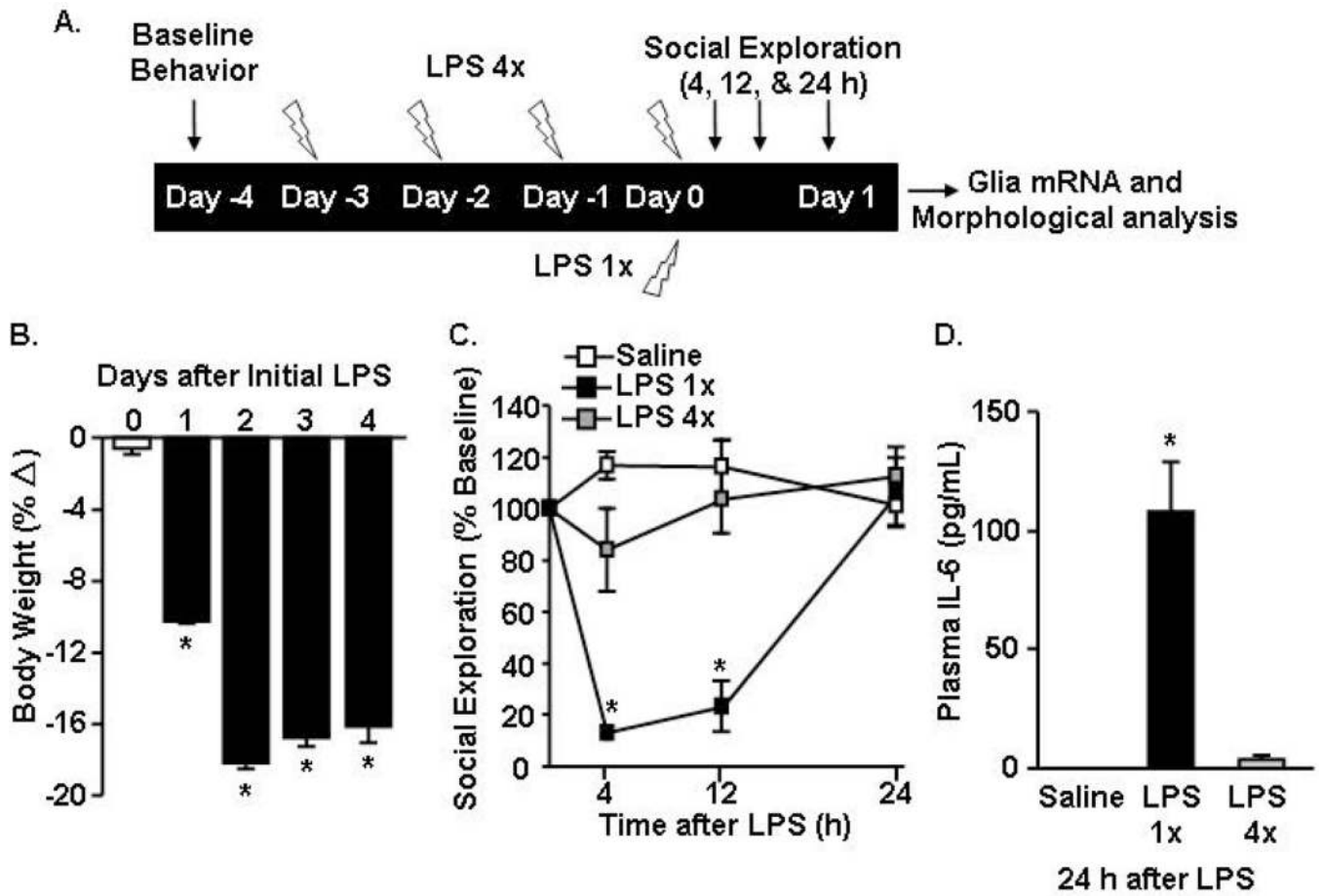
Figure 4. Acute LPS challenge corresponded to a more pronounced active sickness response over 24 h compared to the behavioral response 24 h after the last injection of repeated LPS

A) Experiment schematic injection paradigm for the single- and four repeated-injections of LPS. Adult BALB/c mice were injected i.p. with saline, 1× LPS (20 μg), or 4× LPS (20 μg). In LPS 4× mice, the four repeated LPS injections were provided in 24 h increments. B) Over the LPS 4× injection time course, body weight was determined daily. C) Social exploratory behavior was determined prior to injections and 4–24 h after the last injection of LPS. D) Plasma IL-6 levels were determined at 24 h after the last LPS injection. *$p < 0.05$ from saline.

A. Brain mRNA levels (Fold Δ)				
	24 h	**Saline**	**LPS 1x**	**LPS 4x**
Inflam	*IL-1β*	1.00 ± 0.05	16.1 ± 1.90*	11.1 ± 1.01*‡
	TNFα	1.05 ± 0.14	21.6 ± 2.64*	3.62 ± 0.42‡
Regulatory	*IL-4Rα*	1.01 ± 0.07	2.87 ± 0.10*	1.51 ± 0.12*‡
	YM-1	1.19 ± 0.33	44.1 ± 8.22*	36.5 ± 8.02*
	TGFβ	1.00 ± 0.02	1.37 ± 0.08*	1.23 ± 0.03*
Acute Phase	*Saa3*	1.12 ± 0.21	2318 ± 323*	1585 ± 486*
	CerulP	1.00 ± 0.04	2.19 ± 0.07*	1.23 ± 0.06*‡
	HaptoG	1.20 ± 0.27	13.7 ± 0.83*	16.1 ± 3.32*
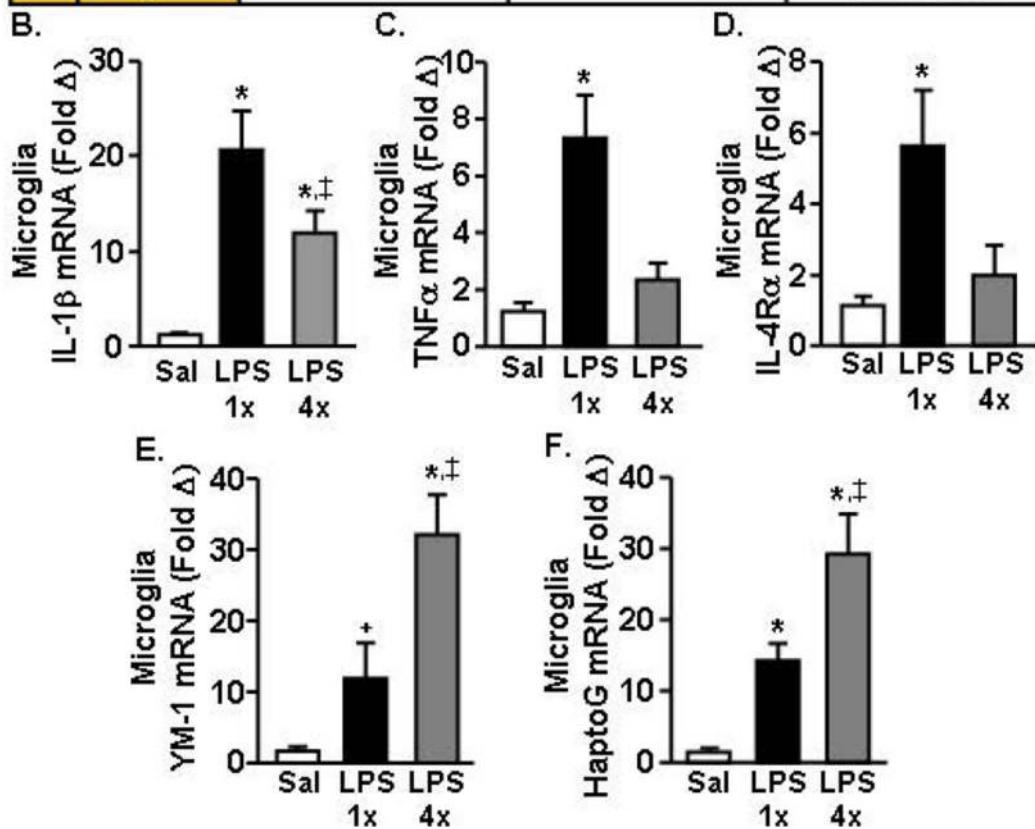
Figure 5. A more pronounced active inflammatory response was evident in the brain 24 h after acute LPS challenge compared to repeated LPS challenge

Adult BALB/c mice were injected (i.p.) with saline, LPS 1× (20 μg), or LPS 4× (20 μg), and a 1 mm coronal brain section was collected 24 h after the last injection. A) mRNA expression of several inflammatory ("Inflam"), "Regulatory," and "Acute Phase" markers were determined. In the same mice, mRNA levels of B) IL-1β, C) TNFα, D) IL-4Rα, E) YM-1, and F) HaptoG were determined in enriched microglia. Means with (*) are different from saline controls ($p<0.05$). Means with (‡) are different from LPS 1× mice ($p<0.05$).
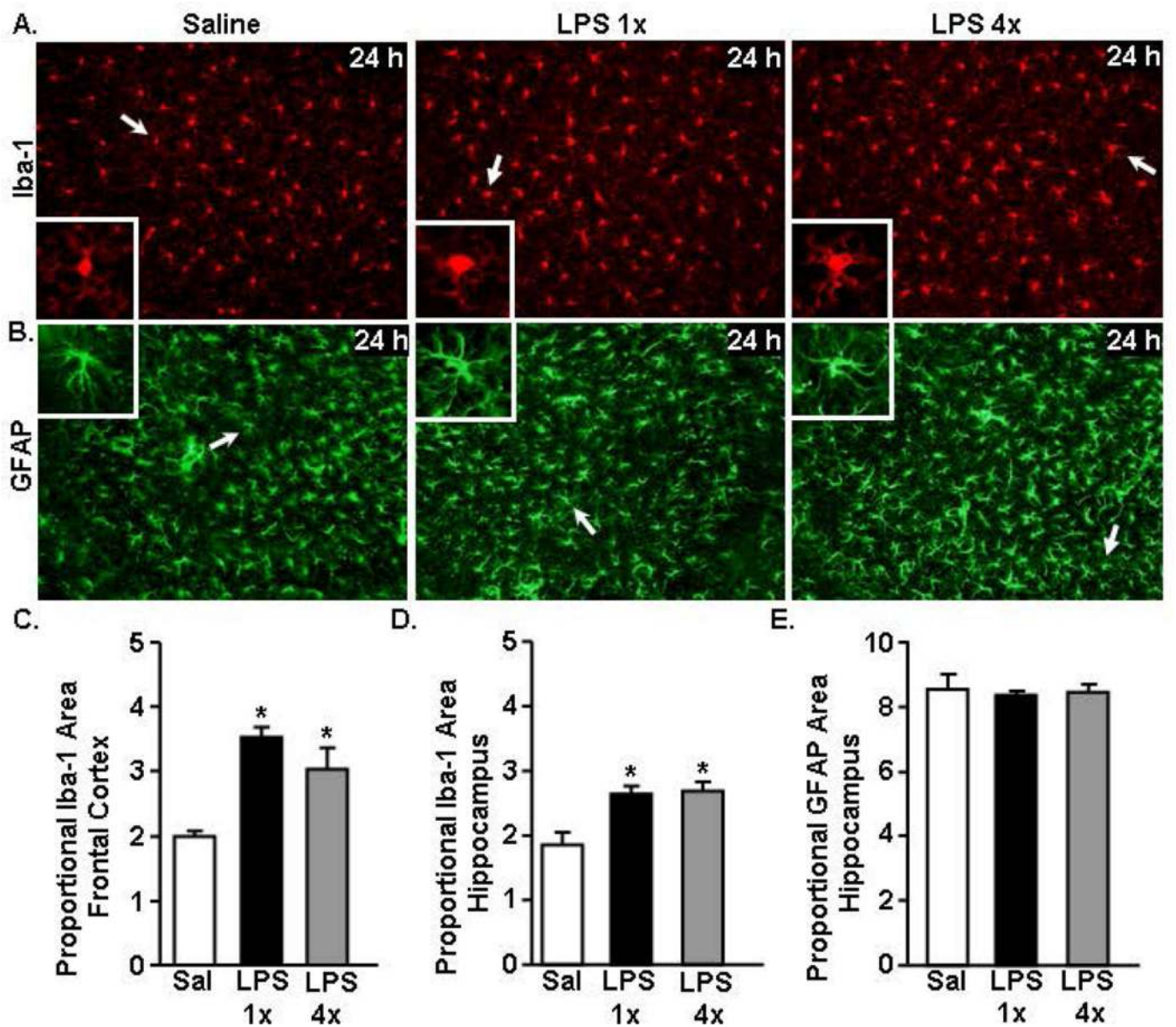
Figure 6. Increased Iba-1 immunoreactivity of microglia 24 h after acute and repeated LPS challenge with no change of GFAP immunoreactivity

Adult BALB/c mice were injected i.p. with saline, LPS 1× (20 μg), or LPS 4× (20 μg). After 24 h, brains were collected and Iba-1 and GFAP immunoreactivity was determined. Representative images of labeling for A) Iba-1 (cortex) and B) GFAP (hippocampus) are shown. White arrows indicate the cell represented in the inset. Proportional area of Iba-1 in the C) frontal cortex and D) hippocampus. E) Proportional area of hippocampal GFAP labeling. $^*p<0.05$ from saline.

Figure 7. Time course of biochemical and morphological alterations of microglial and astrocyte activation in the context of LPS-induced sickness behavior

This illustration summarizes the biochemical and morphological alterations of microglia and astrocytes after peripheral LPS challenge. *Activation:* Microglia were rapidly and robustly activated at 2–4 h after LPS to express cytokines, chemokines and acute phase markers. This microglial activation was associated with a ramified Iba-1 morphology and an active sickness behavioral response. At 2–4 h astrocytes had a down regulation of TGFβ, limited cytokine induction and no alteration in GFAP morphology. *Transition:* By 12 h after LPS, the profile of microglia was attenuated. This change was associated with a ramified Iba-1 morphology and a resolving sickness behavioral response. Astrocytes had a peak activation of cytokine and chemokine expression 12 h after LPS but no alteration in GFAP morphology. *Resolution:* By 24–48 h after LPS microglia had baseline expression of cytokines and chemokines, but also had some level of maintenance of IL-10, YM-1 and acute phase genes in acute and repeated LPS injection. This regulatory profile, however, was augmented by repeated LPS injection. In both cases, microglia resolution was associated with de-ramified Iba-1 morphology and resolved sickness behavior. Astrocytes had an altered gene expression profile after LPS with increased TGFβ, but no changes were detected in their GFAP morphology.

Table 1

Acute LPS challenge induced concomitant induction of inflammatory, regulatory, and acute phase markers in the brain

Adult mice were injected (i.p.) with saline or LPS (10 μg) and a 1 mm coronal brain section was collected 2, 4, 12, 24, and 48 h later. mRNA expression of several "Label", inflammatory ("Inflam"), "Regulatory", and "Acute Phase" markers were determined.

	Gene	Saline	LPS (2 h)	LPS (4 h)	LPS (12 h)	LPS (24 h)	LPS (48 h)
				Brain mRNA levels (Fold Δ)			
Label	Iba-1	1.00 ± 0.06	0.92 ± 0.09	0.94 ± 0.18	0.88 ± 0.04	2.00 ± 0.22*	1.36 ± 0.08+
	GFAP	1.03 ± 0.12	1.22 ± 0.12	1.24 ± 0.08	1.78 ± 0.16*	1.92 ± 0.10*	1.32 ± 0.22
Inflam	IL-1β	1.02 ± 0.09	13.8 ± 1.44*	24.9 ± 3.64*	9.58 ± 2.07*	4.16 ± 0.45	3.78 ± 0.39
	IL-6	1.00 ± 0.05	51.6 ± 12.5*	18.2 ± 1.27*	1.27 ± 0.14	1.10 ± 0.20	0.93 ± 0.05
	TNFα	1.03 ± 0.10	9.08 ± 1.48*	13.6 ± 3.74*	9.43 ± 2.20*	3.54 ± 0.89	2.74 ± 0.57
Regulatory	IL-4Ra	1.04 ± 0.14	1.91 ± 0.14*	4.89 ± 0.55*	2.77 ± 0.46*	1.66 ± 0.13+	1.50 ± 0.12
	IL-10	1.24 ± 0.35	15.9 ± 1.50*	10.5 ± 2.59*	3.29 ± 0.85	2.09 ± 0.48	1.23 ± 0.39
	TGFβ	1.00 ± 0.04	0.89 ± 0.05	0.90 ± 0.07	0.97 ± 0.05	1.36 ± 0.07*	1.41 ± 0.12*
	YM-1	1.37 ± 0.47	1.38 ± 0.26	3.17 ± 0.91	12.3 ± 4.21*	5.54 ± 2.23+	1.06 ± 0.46
Acute Phase	Saa3	1.37 ± 0.47	15.3 ± 3.78	66.3 ± 9.58+	231 ± 97.8*	91.5 ± 16.2*	26.3 ± 7.40
	CerulP	1.02 ± 0.07	2.43 ± 0.21*	3.45 ± 0.47*	2.61 ± 0.41*	1.63 ± 0.19+	1.11 ± 0.13
	HaptoG	1.12 ± 0.21	3.30 ± 0.51	4.99 ± 0.31*	14.38 ± 3.30*	5.60 ± 0.78*	2.23 ± 0.37

Means with (*) are different from saline controls ($p<0.05$) and means with (+) tend to be different from saline controls (p=0.06–0.10).